EFFECT OF AMBIGUITIES ON SAR PICTURE QUALITY

VIJAYA N. KORWAR
DEPARTMENT OF ELECTRICAL ENGINEERING
CALIFORNIA INSTITUTE OF TECHNOLOGY
PASADENA, CALIFORNIA 91125

RICHARD G. LIPES
JET PROPULSION LABORATORY
CALIFORNIA INSTITUTE OF TECHNOLOGY
4800 OAK GROVE DRIVE
PASADENA, CALIFORNIA 91103

SUMMARY

In this paper, we investigate and simulate the degradation of picture quality in a high-resolution, large-swath SAR mapping system caused by speckle, additive white Gaussian noise and range and azimuthal ambiguities occurring because of the non-finite antenna pattern produced by a square aperture antenna. The effect of the azimuth antenna pattern was accounted for by calculating the azimuth ambiguity function. Range ambiguities were accounted for by adding, to each pixel of interest, appropriate pixels at a range separation corresponding to one pulse repetition period, but attenuated by the antenna pattern. A method of estimating the range defocussing effect which arises from the azimuth matched filter being a function of range is shown. The resulting simulated picture was compared with one degraded by speckle and noise but no ambiguities. It is concluded that azimuth ambiguities don't cause any noticeable degradation (for large time bandwidth product systems, at least) but range ambiguities might. However, this latter degradation can also be removed by picture enhancement if the variation of terrain intensity as a function of range is not too great.

1.0 INTRODUCTION

Range and azimuth ambiguities caused by the antenna pattern not being finite degrade the quality of pictures obtainable in an SAR mapping system. So do speckle and white Gaussian noise added by the receiver. When fine azimuthal resolution as well as large range swath are desired, range ambiguities become serious. We consider the worst case where the swath is so large that the time between successive pulses is just sufficient to accomodate the

return from the terrain between the 6 dB points of the antenna range pattern. A square antenna aperture is assumed, so the two-way antenna amplitude pattern is a $(\text{sinc})^2$ function for both range and azimuth. Thus, the first sidelobe is about 26 dB down below the main lobe and the response from pixels lying outside the mainlobe are considered negligible. The points halfway between the beam direction and the first zero of the $(\text{sinc})^2$ function have an amplitude of $(\frac{2}{\pi})^2$ which is approximately 1/2, so the 6 dB beamwidth was, for simplicity, considered to be half the width between the first zeros on either side. A lunar picture of 256 (azimuth) x 512 (range) 8-bit pixels was taken and each pixel degraded as described below. Each pixel is assumed to correspond to a just-resolvable square cell. First, each pixel intensity was replaced by a pair of Gaussian random variables to account for speckle and additive white noise. The azimuth ambiguity was accounted for by calculating the azimuth ambiguity function and superposing it on the picture. Range ambiguities occur because of returns from previous and succeeding pulses not being sufficiently attenuated by the antenna pattern. These were suitably added. The process of generating random numbers and adding appropriate multiples of ambiguous pixels was repeated for 40 looks and the final picture compared with one having speckle and noise but no ambiguities. Range curvature and the effects of rotation of the terrain were neglected.

2.0 THE SIMULATION

2.1 SPECKLE AND NOISE

According to the model developed by Butman and Lipes [1], a given pixel is formed by envelope-detecting an in-phase and quadrature signal which are contaminated by receiver noise, so that each pixel is represented by I and Q components

$$V_I = a_I + n_I \tag{1}$$

$$V_Q = a_Q + n_Q \tag{2}$$

where a_I, a_Q = I and Q components of voltages in the pixel in the absence of noise and

n_I, n_Q = noise voltages

All four are statistically independent (S.I.) zero-mean Gaussian random variables (G rvs) with a_I, a_Q being identically distributed with variance = $\frac{1}{2}$ x pixel intensity and n_I, n_Q being identically distributed with variance = $\frac{1}{2}$ x noise power. The pixel power that is obtained after correlation is

$$p_i = v_I^2 + v_Q^2 \tag{3}$$

which is an estimate of the actual pixel power

$$s = a_I^2 + a_Q^2 \tag{4}$$

After M looks the estimate of pixel power is

$$p = \frac{1}{M} \sum_{i=1}^{M} p_i \tag{5}$$

2.2 AZIMUTH AMBIGUITIES

Let $\sigma(x)$ describe the complex reflectivity of the ground as a function of position x of the spacecraft at slant range r_o and let the wavelength be λ. Then the signal return obtained after heterodyning with the carrier is

$$O(x) = \int_{-\infty}^{\infty} \sigma(x')\ C(x-x')\ A(x-x')dx' \tag{6}$$

where

$$C(x) = e^{2\pi i \frac{x^2}{r_o \lambda}} \tag{7}$$

$$\begin{aligned} A(x) &= \text{azimuth antenna pattern} \\ &= \{(\sin H(x))/H(x)\}^2 \end{aligned} \tag{8}$$

and

$$H(x) = \frac{\pi D}{\lambda} \cdot \frac{x}{r_o} (1+x^2/r_o^2)^{-\frac{1}{2}}$$

where D = length (or width) of antenna aperture.

The output after matched filtering is

$$G(x) = \int_{-\infty}^{\infty} O(x+x'')\ C(x'')\ A(x'')\ dx''$$

$$= \int_{-\infty}^{\infty}\int_{-\infty}^{\infty} \sigma(x')\ C(x''+x-x')\ A(x''+x-x')\ C(x'')\ A(x'')\ dx'dx''$$

$$= \int_{-\infty}^{\infty} \sigma(x')\ \rho(x-x')\ dx' \qquad (9)$$

where $\rho(\tau)$ is the correlation function of the A(x) C(x), i.e. of the azimuth chirp modulated by the two-way antenna pattern which is a $(\text{sinc})^2$ function. (This latter function is hereafter referred to as the chirp $(\text{sinc})^2$ function.)

The correlation function $\rho(x)$ can be calculated by two methods:

(a) the method of stationary phase

(b) computer simulation

For method (a) we consider $x/r_o << 1$ and prop. 2.19, p. 45 of [3] which gives the power spectrum of

$$f(x) = e^{-2\pi i x^2/r_o\lambda}\left(\frac{\sin(\frac{\pi Dx}{\lambda r_o})}{\frac{\pi Dx}{\lambda r_o}}\right)^2 = e^{-\frac{1}{2}ikx^2}\left(\frac{\sin \alpha x}{\alpha x}\right)^2 \qquad (10)$$

$$\text{as } |F(\omega)| \quad \frac{2\pi}{k}\ \frac{\sin \frac{\alpha\omega}{k}}{\frac{\alpha\omega}{k}}^4 \qquad (11,$$

for the large time bandwidth product (TBP) case. The inverse of this is the correlation function of f(x) which can be calculated in closed form and is

$$\rho(\tau) = \frac{2}{3}\frac{D^3}{8} - \tau^2\frac{D}{2} + \frac{\tau^3}{2} \qquad (0 \le |\tau| \le \frac{D}{2})$$

$$\frac{-\tau^3}{6} + \tau^2\frac{D}{2} - \frac{D^2}{2}\tau = \frac{D^3}{6} \qquad (\frac{D}{2} < |\tau| < D) \qquad (.2)$$

and is shown in Fig. 2, after normalizing to $\rho(0) = 1$. Method (b), in which the function f(x) was replaced by its main lobe only and sampled every D/4. In this case, the approximation $x << r_o$ was dropped (it is not really valid

for large swath). Computer calculation of $\rho(\tau)$ was done for TBP's of 256 and 200,000 and in each case the resulting plot is very close to Fig. 2 with $\rho(\tau)$ falling below 10^{-6} after $\tau = D$.

To allow for the possibility that the correlation function used will be a rect chirp instead of a $(\text{sinc})^2$ chirp, the cross-correlation function of these two was evaluated by methods (a) and (b). So was the auto-correlation function of the rect chirp. This latter is itself a sinc function with zero at $\tau = D/2$ as expected while the cross-correlation of the rect and sinc chirps is intermediate in shape between the auto-correlation functions of the rect chirp and $(\text{sinc})^2$ chirp. Remembering that the basic azimuth resolution cell is of width D/2, it seems that in no case do pixels beyond the first on either side of a pixel of interest contribute to the return for that pixel.

The fraction of the adjacent pixel which must be added to the pixel of interest is calculated as follows:
Consider the signal returns from the ground to be discretised with one return intensity accounting for each resolution cell. The I (or Q) component of a signal return is assumed to be

$$z_{ij} = y_{ij} + \alpha(y_{i+1,j} + y_{i-1,j}) \tag{13}$$

for the pixel in the ith azimuth and jth range; y_{ij} is the actual Gaussian random variable for this element and α is an appropriate weight. Similarly,

$$z_{i+1,j} = y_{i+1,j} + \alpha(y_{i+2,j} + y_{ij}) \tag{14}$$

Since all the y's with different subscripts are independent,

$$\overline{z_{ij} z_{i+1,j}} = \alpha(\overline{y_i^2}) + \alpha(\overline{y_{i+1}^2}) \approx 2\alpha\overline{y_i^2} \tag{15}$$

where bars denote expected value and we assume the intensity of ijth and (i+1)j th pixel is approximately the same

$$\overline{z_i^2} = \alpha^2 \overline{y_i^2} + (\overline{y}_{i+1}^2 + \overline{y}_{i-1}^2) \approx (\alpha^2 + 2)\overline{y_i^2} \tag{16}$$

This means the ratio of the correlation between adjacent elements in the picture to the power of the pixel itself is

$$R = \frac{2\alpha}{\alpha^2 + 2} \tag{17}$$

To evaluate σ using the correlation function $\rho(\tau)$ calculated before, we consider the correlated output for the continuous model of the ground (Eq.(9))

$$G(x) = \int_{-\infty}^{\infty} \sigma(x')\ \rho(x - x')dx' \tag{9}$$

We have for the correlation function of G(x),

$$\begin{aligned} R(x - y) &= \overline{G(x)\ G^*(y)} \\ &= \iint_{-\infty}^{\infty} \overline{\sigma(x')\sigma^*(y')}\ \rho(x-x')\ \rho^*(y-y')\ dx'dy' \qquad (18) \\ &\approx \int_{-\infty}^{\infty} dx' \overline{|\sigma(x')|^2}\ \rho(x-x')\ \rho^*(y-x') \end{aligned}$$

because $\sigma(x')$ and $\sigma(y')$ are S.I., so that

$$\overline{\sigma(x')\ \sigma^*(y')} = |\sigma(x')|^2\ \delta(x'-y') \tag{19}$$

Now $\rho(x-x')$ and $\rho^*(y-x')$ have a very short extent so that unless x and y are close, the integral in (18) is zero. If x and y are close, the integral over x' is nonzero only over a short distance so that $\overline{|\sigma(x')|^2}$ is approximately constant = σ^2.

$$\begin{aligned} \therefore\ R(x - y) &= \sigma^2 \int_{-\infty}^{\infty} dx'\ \rho(x-x')\ \rho^*(y-x') \\ &= \sigma^2 \int_{-\infty}^{\infty} dz\ \rho(\tau)\ \rho^*(z+x-y) \qquad (20) \\ &= \sigma^2\ a(x-y) \end{aligned}$$

where $a(\tau)$ is the autocorrelation function of $\rho(\tau)$.

Now if a pixel extends from -D/4 to D/4, its adjacent one extends from D/4 to 3D/4, so it is centered at D/2. Thus, if x-y = D/2, $\frac{R(D/2)}{R(0)}$ represents the same ratio as R in Eq. (17).

$$\frac{R(D/2)}{R(0)} = \frac{\sigma^2 a(D/2)}{\sigma^2 a(0)} = \frac{a(D/2)}{a(0)} \tag{21}$$

From Eqs. (17) and (21),

$$\frac{a(D/2)}{a(0)} = \frac{2\alpha}{\alpha^2+2} \tag{22}$$

$\frac{a(D/2)}{a(0)}$ can be evaluated for the chirp $(\text{sinc})^2$ by finding the correlation function of Fig. 2 and is equal to 0.493.

$$\therefore \quad 0.493 = \frac{2\alpha}{\alpha^2+2} \tag{23}$$

$$\text{or} \quad \alpha = 0.268 \tag{24}$$

for the chirp $(\text{sinc})^2$ function. This is the required weight factor for adjacent pixels in azimuth. The weight factor required if a rect chirp were used in the matched filtering can be similarly calculated but was smaller than 0.268. So in the simulation the worst-case of $\alpha = 0.268$ was used.

2.2 RANGE AMBIGUITIES AND RANGE DEFOCUSSING

No chirp or coding was assumed for the range direction, so adjacent range bins don't contribute to the ambiguity as in the azimuth case. However, there is a more serious effect in this case, because one pulse on either side of the pulse of interest (corresponding to a range bin of interest) is quite intense because it lies in the mainlobe of the antenna range pattern, though outside the central half. Since only the mainlobe is considered, this means that for each range bin there is exactly one range bin that contributes an ambiguity as shown in Fig. 1. The central 256 bins form the desired swath while the ambiguous range bin corresponding to the ith bin is the one at (i + 256) mod (512). Thus R1' is the ambiguous bin corresponding to R1, and R2' corresponds to R2. We say this kind of ambiguity is more serious than the azimuth type (or the type that would additionally be present in range if range coding or range chirp were used) because while adjacent pixel powers don't vary much, those separated by 256 range bins do.

There is, however, a mitigating effect: each pixel is affected by not just one, but several pixels in the ambiguous range bin. This is because the azimuthal ambiguity function is a function of range that extends over several elements at the ambiguous range bin. If it did not do so, each pixel in the ith range bin would have just the pixel in its azimuthal line in the (i + 256) mod (512) range bin adding to it and the variation with azimuth of the pixel intensity in the latter range bin would cause widely

varying numbers to be added to the pixel in the ith range bin. The mitigating effect can be calculated as follows (in this calculation, the $(\text{sinc})^2$ modulation in azimuth was neglected). The return from the ambiguous range bin at range r_1 is of the form $e^{-2\pi i\, x^2/r_1\lambda}$ while the azimuth matched filter for the desired range bin at range r_o is $e^{-2\pi i\, x^2/r_o\lambda}$. The magnitude of the cross-correlation function

$$r(\tau) = \left| e^{-2\pi i\, x^2/r_1\lambda} * e^{-2\pi i\, x^2/r_o\lambda} \right| \tag{25}$$

was evaluated by computer and found to be fairly constant over its extent, though the phase varies rapidly. This rapid phase variation allows another simplification to be made in the simulation: to be accurate, the I and Q random variables for the various elements in the ambiguous range bin weighted by the corresponding components of the cross-correlation function should have been added to the I and Q components of the desired pixel. But this is time-consuming. However, because of the rapid phase variation of $r(\tau)$, this entire process of weighting and summing was replaced by generating just two random variables with zero mean and with variance equal to the sum of the powers of all pixels in a range bin contributing to the ambiguity for a given pixel. That is, if $y_{ik\,I}$ and $y_{ik\,Q}$ are the I and Q components of a pixel of interest, the range ambiguity was represented by adding two S.I. zero mean Gaussian random variables each of variance $\frac{1}{2} T_{i'k}$

$$\tfrac{1}{2} T_{i'k} = \tfrac{1}{2} a_{i'} \Sigma_k c_k p_{i'k} \tag{26}$$

where c_k = squared magnitude of cross-correlation coefficients (i.e., samples of $r^2(\tau)$)

$p_{i'k}$ = powers of pixels in the ambiguous (i'th) range bin contributing to range ambiguity for p_{ik}

and $a_{i'}$ = the attenuation due to the antenna range pattern at the i'th range.

The further approximation made is that the c_k are all equal, which is what the computer calculation of $r(\tau)$ indicates. These simplifications seem justifiable because the resulting pictures seem insensitive to just how many pixels $r(\tau)$ extends over, as long as the area under the $r^2(\tau)$ is kept the same. In the simulated pictures attached (Fig. 3), set III corresponds to the case where $r(\tau)$ extends over 15 elements and set II to that where $r(\tau)$

extends over 7 elements, but otherwise similar. In addition computer print-outs for one range bin were obtained for $r(\tau)$ spread over 25 and 51 elements and were all seen to be very close.

Another result that is obtained from the computer calculation of $r(\tau)$ is that the area under $r^2(\tau)$ is the same as that under the autocorrelation function of the chirp rect, which is normalized to 1. This is to be expected since correlating $e^{-2\pi i x^2/r_o\lambda}$ with $e^{-2\pi i x^2/r_1\lambda}$ merely spreads the energy of return over several pixels in the ambiguous range instead of focussing it into one pixel as it does if $r_1 = r_o$. Thus, all that needs to be calculated if a quick estimation of $T_{i'k}$ is required without a computer is to find the number n of elements $r(\tau)$ spreads over; then c_k is 1/n. A quick estimate can be obtained as follows:

Let v = velocity of spacecraft = $\frac{x}{t}$

T = time for which the rectangular chirp lasts = $\frac{L}{v}$ (27)

where L = synthetic aperture length = $\frac{\lambda r_o}{D}$

Let $k_o = \frac{2\pi v^2}{r_o\lambda}$, $k_1 = \frac{2\pi v^2}{r_1\lambda}$, (28)

$$\therefore\ r(\tau) = e^{-ik_o t^2} * e^{-ik_1 t^2}$$

$$= \int_{-T/2}^{T/2-|\tau|} e^{ik_o(t+\tau)^2}\, e^{-ik_1 t^2}\, dt$$

$$= e^{ik_o\tau^2} \int_{-T/2}^{T/2-|\tau|} e^{i(k_o-k_1)t^2}\, e^{i2k_o t\tau} dt \qquad (29)$$

which can be reduced to give

$$|r(\tau)|^2 = fc^2 + fs^2 \qquad (30)$$

where

$$fc = \frac{1}{\alpha}\int_{\alpha\left[-T/2 + k_o\tau/(k_o-k_1)\right]}^{\alpha\left[T/2 + k_o\tau/(k_o-k_1)\right]} \cos\left(\frac{\pi x^2}{2}\right) dx \qquad (31)$$

$$fs = \frac{1}{\alpha}\int_{\alpha\left[-T/2 + k_o\tau/(k_o-k_1)\right]}^{\alpha\left[T/2 + k_o\tau/(k_o-k_1)\right]} \sin\left(\frac{\pi x^2}{2}\right) dx \qquad (32)$$

$$\alpha = \sqrt{\frac{4v^2}{\lambda}\left(\frac{1}{r_o} - \frac{1}{r_1}\right)} \tag{33}$$

It can be seen from tables of Fresnel integrals, that fc^2 and fs^2 are almost constant until both upper and lower limits of integration are > about 4. and then fc^2 and fs^2 start falling.

Thus, $|r(\tau)|^2$ is negligible when

$$\alpha\left(\tau \frac{k_o}{k_o - k_1} - \frac{T}{4}\right) \simeq 4 \tag{34}$$

Solving

$$\frac{k_o}{k_o - k_1} = \frac{\frac{1}{r_o}}{\frac{1}{r_o} - \frac{1}{r_1}} \simeq \frac{r_o}{\Delta r} \tag{35}$$

and the time bandwidth product

$$TBP = \frac{L}{D/2} = \frac{vT}{v\tau_o} = \frac{T}{\tau_o} \tag{36}$$

where $\tau_o = D/2v$ = time between successive pulses (37)

we get for the number of elements (of length D/2) on each side that $r(\tau)$ extends over,

$$\frac{\tau}{\tau_o} = \frac{\Delta r}{r_o} \cdot \frac{T}{2} \cdot \frac{1}{\tau_o} + \frac{4}{\alpha} \cdot \frac{\Delta r}{r} \cdot \frac{1}{\tau_o}$$

$$= \frac{\Delta r}{r_o}\left[\frac{TBP}{2}\right] + \sqrt{\frac{8}{TBP}}\sqrt{\frac{\Delta r}{r_o}} \tag{38}$$

For large TBP only the first term on the right of Eq. (38) needs to be retained. For the simulation, TBP = 256 and we get $\tau/\tau_o = 6$ so that $r(\tau)$ extends over 12 elements on either side of a central one or n = 12 + 1 = 13 elements in all. The computer calculation of $r(\tau)$ gives n = 15.

2.3 OBTAINING THE PICTURES

The simulation was performed by

(i) generating two zero-mean S.I. G rvs for each of the 256 x 256 pixels of interest, with variances equal to ½ the pixel intensity x the range antenna function for the pixel;

(ii) generating two S.I. zero mean G rvs with correct variance

corresponding to range ambiguity, Eq. (26) and adding to the values in (i) above;

(iii) adding the I and Q G rvs respectively of one adjacent pixel on each side with $\alpha = 0.268$ for the azimuth ambiguity, Eq. (24); at this stage the G rvs correspond to a_I and a_Q in Eqs. (1), (2);

(iv) generating two G rvs corresponding to n_I and n_Q, with variance $N_o = 10$ on a 0 - 255 intensity scale (this value of N_o was chosen by finding the mean picture intensity to be 50 and requiring an SNR of 5); we now have v_I and v_Q of Eqs. (1) and (2);

(v) squaring and adding v_I and v_Q to get p_i(Eq. (3));

(vi) repeating (i) to (v) 40 times and averaging p_i to get p of Eq. (5).

Additive white noise N_o merely translates the distribution curve of pixel intensities in the original picture by an amount equal to the noise power, provided the noise is not so large that the variance it introduces into v_I and v_Q is not averaged out by the number of looks taken. By subtracting that value of pixel power in the output below which lie less than 5% of the pixels(in the output picture so far obtained), the noise is effectively removed. In addition, the contrast of the picture was increased by 'stretching' the range of intensities occupied by the picture (both the original and the simulated ones) to extend over as much of the 0 - 255 range as possible.

3.0 PROCESSING AND RESULTS

See Fig. 3. Pictures (a) and (b) are the 256 x 512 original and the 256 x 256 original. The other 9 pictures are divided into sets of 3, each set being in one horizontal line. The topmost, set I, was obtained without azimuth or range ambiguities being added, but the antenna range pattern is superposed on the picture; speckle and noise are present in the picture; i.e., it was obtained as in 2.3 but with $\alpha = 0$ and $T_{i',j} = 0$ in Eq. (26). Sets II and III do have azimuth and range ambiguities as well as speckle and noise; the only difference is that Set II had the range ambiguity spread over 7 elements (n = 7) while set III had n = 15. There is no visible difference between the corresponding pictures of these two sets.

In each set, the left most picture, i.e. (c), (f), (i), was obtained as

described above; the second and third pictures of each set have additional enhancement techniques applied. We notice that all 9 pictures are worse than the original because of speckle, but that major features are still recognizable in the central portions of all of them. However, the upper and lower edges, corresponding to the ends of the range swath, in (c), (f), (i) show the effect of the antenna range pattern attenuation and it is very difficult to distinguish craters and so on in these regions. However, (f) and (i) are almost as good as (a) in recognizability of features showing that ambiguities don't make much difference to the picture quality if further enhancement is not used, because the edges, where range ambiguities are most important, are attenuated in all three sets.

The second picture of each set, i.e. (d), (g), (j), was obtained by dividing each pixel power after 40 looks by the approximate antenna range pattern attenuation, and then subtracting white noise and 'stretching.' In all three cases, the edges now appear too bright--this is because the range ambiguity plus white noise at the edges are now enhanced and distinguishing features at the edges is just as difficult as in (c), (f), and (i).

The third picture of set I, i.e. (e), was obtained by first subtracting the white noise, i.e. 10 on a 0 - 255 scale, from each pixel power after 40 looks and then dividing by the antenna range attenuation function. Then the picture was 'stretched.' Now it is possible to see more features at the edges than before.

In the third pictures of sets II and III, i.e. (h) and (k), the white noise of 10 plus an estimate of range ambiguity was subtracted from each pixel and then this was divided by the antenna range attenuation factor and stretched. The estimate of range ambiguity used was equal to the average picture intensity (= 50) times the antenna pattern attenuation at the ambiguous range bin. In all these pictures, i.e. (e), (h) and (k), the edges are now not too bright or dim and, in addition, (h) and (k) are almost indistinguishable from (e).

4.0 CONCLUSIONS

(i) The effect of azimuth ambiguities seems to be negligible in the pictures since the central areas, where range ambiguities are not important,

are not noticeably different in sets I, II and III. This is expected from the fact that only adjacent pixels contribute to the ambiguity.

(ii) The effect of range ambiguities, for the particular picture used here, is more or less removable by enhancement techniques, because the intensity of the ambiguous ranges is not too different from the mean picture intensity. But this could easily not be the case and then, since the correct estimate of ambiguity is not available, the enhancement won't improve quality very much.

(iii) Speckle is the major source of picture degradation, as can be seen from the fact that the pictures with speckle and no ambiguities are noticeably worse than the original, while the pictures with ambiguities and speckle are not too different from those without ambiguities but with speckle.

5.0 OTHER POSSIBILITIES

One way to bring the mean intensity of pixels contributing to range ambiguities nearer to the mean picture level is by spreading the energy in the ambiguous return over more elements. (Then the enhancement technique described can be used to remove the ambiguities.) This can be done by using equal chirps of opposite sign on alternate pulses so that they don't correlate. Another way, suggested by Dr. J. R. Pierce, is to use opposite directions of circular polarization on alternate pulses. This method, in fact, even reduces the total energy from ambiguous returns, as long as the ground reflects the signal back more or less circularly polarized.

6.0 ACKNOWLEDGEMENTS

The authors are grateful to Dr. J. R. Pierce for his suggestion.

7.0 REFERENCES

1. Butman, S. A. and Lipes, R. G., "The effect of noise and diversity on SAR imagery," Deep Space Network Progress Report 42-29, Jet Propulsion Laboratory, Pasadena, California, July and Aug. 1975, p. 46.

2. Harger, R. O., Synthetic Aperture Radar Systems: theory and design, Academic Press, 1970.

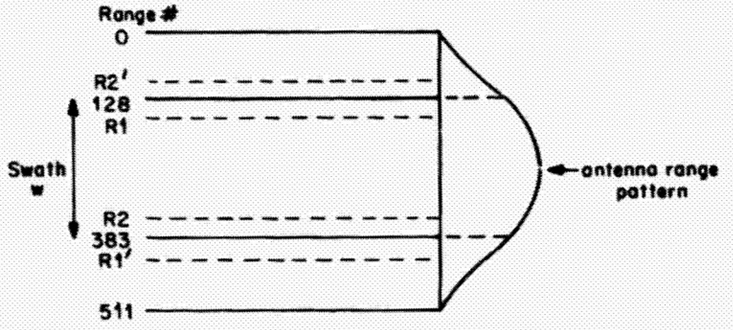

FIG. 1 ILLUSTRATING RANGE AMBIGUITIES

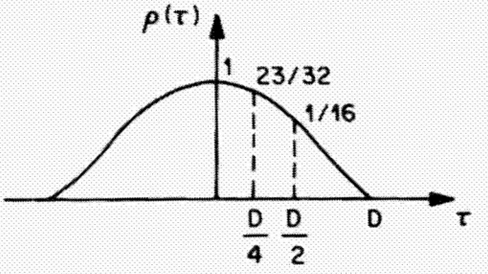

FIG. 2 CORRELATION FUNCTION FOR CHIRP $(S..C)^2$ FUNCTION

(a)

(b)

FIG. 3 (a) AND (b): ORIGINAL PICTURES OF A LUNAR SCENE.

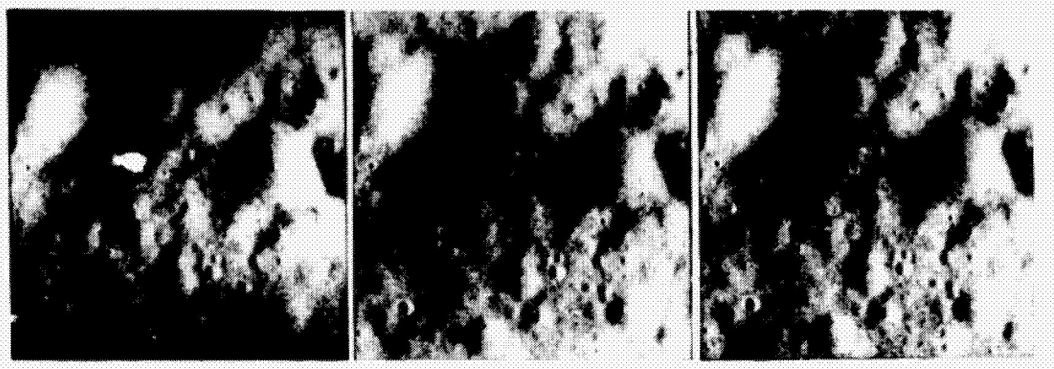

(c) (d) (e)

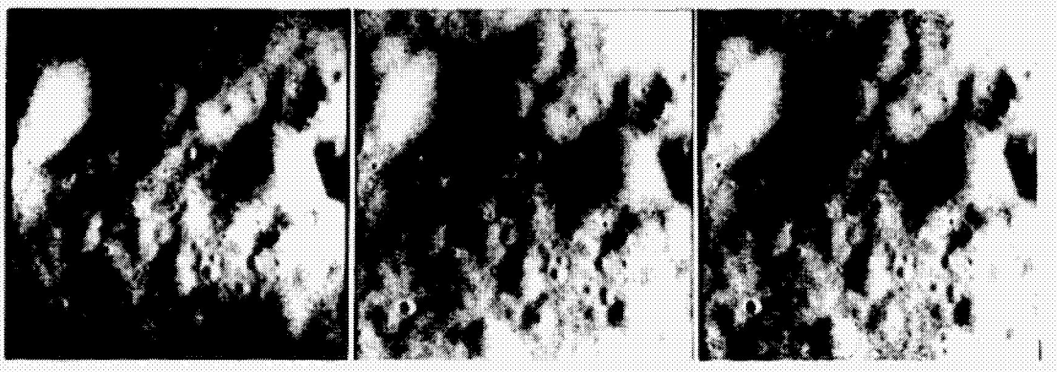

(f) (g) (h)

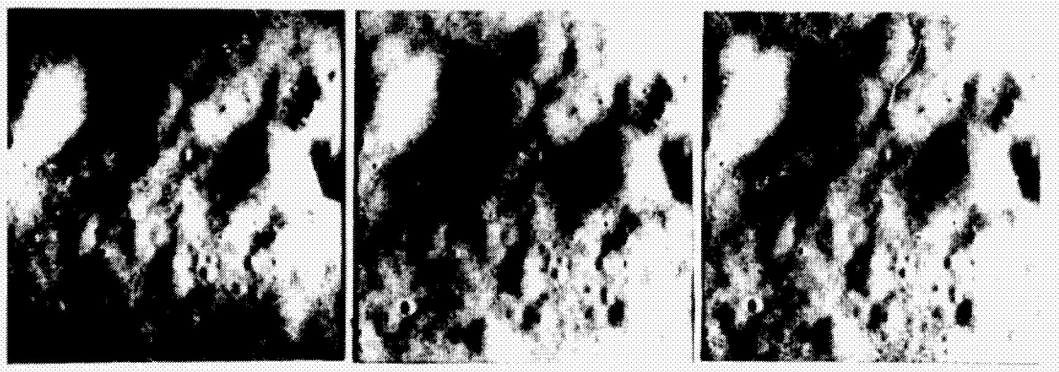

(i) (j) (k)

FIG 3 (c) THROUGH (k): SIMULATED PICTURES OF THE SAME SCENE.